

Synthesis of bio-functionalized copolymer particles bearing carboxyl groups via a microfluidic device

Shih Hao Huang · Hwa Seng Khoo ·
Shang Yu ChangChien · Fan Gang Tseng

Received: 23 January 2008 / Accepted: 12 March 2008 / Published online: 2 April 2008
© Springer-Verlag 2008

Abstract Monodisperse copolymer particles carrying surface carboxyl groups in the range of 50–200 μm were prepared by in situ UV polymerization of ethyleneglycol dimethacrylate (EGDMA) with acrylic acid (AA) via a microfluidic flow-focusing device (MFFD). The design of the coaxial orifices in the MFFD enables the confinement of the comonomer liquid thread to the central axis of the microchannel, which can avoid the wetting problem of comonomer liquid with the microchannel and can successfully produce monodisperse copolymer microspheres with coefficient of variance below 5%. The effects of concentration of EGDMA and AA on droplet diameters and the distribution of carboxyl group on particle surfaces were examined. It has been found that, increasing the concentration of AA would decrease particle sizes, but increase the distribution of carboxyl group on particle surfaces. Bioconjugation of the carboxylated copolymer particles with the anti-rabbit IgG–Cy3 conjugates was successfully demonstrated. By increasing the concentration of AA accompanied with decreasing the particle sizes, high efficiency of bioconjugation on carboxylated copolymer particles was achieved. The rapid continuous synthesis of carboxylated copolymer particles via a microfluidic device

provides a reliable control of particle sizes and composition for massive production in biotechnological applications.

Keywords Flow-focusing device · Copolymer · EGDMA/AA · Bioconjugation

1 Introduction

Recently, functional groups-carrying micron-size uniform polymer particles have attracted attention in the area of the biotechnological and biomedical applications, such as affinity chromatography, immobilization technologies, drug delivery systems, and cell culturing (Rembaum and Toke 1998; Slomkowski 1998; Kawaguchi 2000; Seong et al. 2003). Detection, immobilization, and separation of DNA, cells, and proteins require particles carrying surface functionalities, e.g., carboxyl, hydroxyl, amine, amide and chloromethyl groups. Among them, the incorporation of carboxyl groups has attracted large attention since the carboxyl groups on particles surfaces can be easily activated for various applications. Polymer particles within the size range of 50 nm–2 μm can be produced by various manufacturing processes including suspension, emulsion, and dispersion polymerizations, etc. (Arshady 1992, 1993; Kesenci and Kin 1998; Zhang et al. 2005). However, these methods are frequently time-consuming, and lack sufficient control over particle size distribution and particle compositions.

A microfluidic-based method (Nisisako et al. 2004, 2006, 2007; Dendukuri et al. 2005; Nie et al. 2005, 2006; Seo et al. 2005a, b; Nisisako et al. 2006) for the rapid continuous in situ photopolymerization of monomer droplets emulsified in a microfluidic flow-focusing device (MFFD) has been proposed and proven to enable the

S. H. Huang (✉)
Department of Mechanical and Mechatronic Engineering,
National Taiwan Ocean University, No.2, Beining Rd,
Keelung 202-24, Taiwan
e-mail: shihhao@mail.ntou.edu.tw

H. S. Khoo · S. Y. ChangChien · F. G. Tseng
Department of Engineering and System Science,
National Tsing Hua University, Hsinchu 30013, Taiwan

F. G. Tseng
Division of Mechanics, Research Center for Applied Sciences,
Academia Sinica, Taipei 115, Taiwan, ROC

generation of extremely monodispersed polymer particles. Typically, the 2D MFFDs composed by polydimethyl siloxane (PDMS) microchannels on glass substrates were extensively used to produce polymer particles. However, wetting properties associated with both liquids and microchannels for current 2D MFFDs are a vital issue in the generating process of monomer droplets. This indicates that the wetting of the channel surfaces, i.e. hydrophobicity and hydrophilicity, has a significant effect on the type of dispersion that can be produced (Seo et al. 2005a). We have found that the liquid thread of ethyleneglycol dimethacrylate (EGDMA) in water solution tends to stick on the channel wall without droplet breakup for the 2D MFFD (Fig. 1b). This is due to the factor that EGDMA has a high affinity with the hydrophobic PDMS channel surfaces. Utilizing the material of polyurethane (PU) elastomer to fabricate the 2D-MFFDs (Nie et al. 2005; Seo et al. 2005b) or coating chemical compounds onto the channel surfaces to modify the surface properties with hydrophilic properties (Okushima et al. 2004) can also probably solve this problem. However, the complex synthesis of the PU elastomer and contamination of chemical compounds limit the practical applications in the massive production. In principle, the wetting phenomenon could be solved by using a 2D-MFFD fabricated in naturally-hydrophilic material such as glass and silicon, which have been used for the formation of monodisperse oil-in-water emulsions and polymeric microparticles (Nisisako et al. 2002, 2004, 2006, 2007). The possibility to produce copolymer microparticles, which could change the wetting property, i.e. hydrophobicity and hydrophilicity, depend on the comonomer composition has not yet been demonstrated using the same device in the literature. To avoid wetting of the channel wall by the dispensed phase, axisymmetric flow-focusing device (AFFD) is a promising technique as the inner dispensed phase is surrounded by the continuous phase and never touches the wall (Loscerales et al. 2002; Banderas et al. 2005; Jeong et al. 2005; Takeuchi et al. 2005; Utada et al. 2005; Oh et al. 2006). In our previous study (Huang et al. 2006), we fabricated a monolithically planar 3D MFFD utilizing three layers of SU-8 resist structures to form coaxial orifices. We successfully demonstrated the formation of highly monodisperse water-in-oil (W/O) and oil-in-water (O/W) droplets as well as micron-size cross-linked microspheres with no functional groups utilizing the same device. However, such configurations need a complicated multilayer fabrication technique to form coaxial orifices. A clamped facility is also needed to seal the channel for the closed channel configuration, limiting the possibility for mass production. Besides, the possibility to produce the bio-functionalized microspheres, i.e. bioconjugation of the microspheres with antibody using the planar 3D MFFD has not yet been demonstrated.

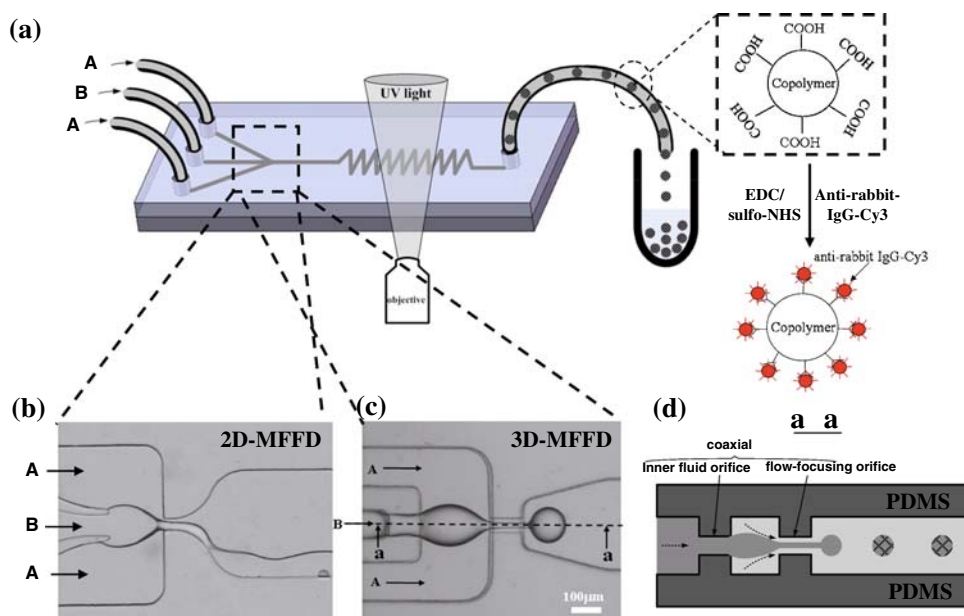
The synthesis of monodisperse copolymer microparticles composed of tripropylene glycol diacrylate (TPGDA) and acrylic acid (AA) using a 2D PU-based MFFD was previously proposed (Lewis et al. 2005). However, only limited composition of comonomer solutions, i.e. TPGDA with $C_{AA}(\text{wt.}\%) < 8\%$ was successfully used to produce into droplets. For $C_{AA}(\text{wt.}\%) > 15 \text{ wt.}\%$, the monomer thread did not break up into droplets. This is due to the fact that AA is a water-soluble monomer with the hydrophilic property. Increasing the concentration (wt.%) of AA can gradually change the property of comonomer solutions from hydrophobic to hydrophilic property, which can lead to the occurrence of wetting phenomenon. In terms of 2D-MFFDs, it is difficult to utilize the same device for the formation of copolymer microparticles composed of different compositions of the comonomer liquids which can significantly change the liquid property. Besides, the copolymer microparticles with insufficient concentration of AA, i.e. $C_{AA}(\text{wt.}\%) < 8\%$, could significantly influence the distribution of carboxyl group on particle surfaces as well as the efficiency of bioconjugation.

In this study, we fabricated a planar 3D MFFD utilizing PDMS with a simplified fabrication process, which can produce monodisperse bio-functionalized copolymer particles composed of EGDMA with $C_{AA}(\text{wt.}\%) = 0, 10, 20, 40\%$ using the same device. High efficiency of bioconjugation on carboxylated copolymer particles was successfully demonstrated by increasing the concentration of AA. The proposed 3D-MFFD with coaxial orifices, which can confine the comonomer liquid thread to the central axis of the microchannel, can overcome the wetting problems. The generation of copolymer particles from a mixture of two monomers of EGDMA (a host monomer) with the acrylic acid (AA) following by in situ UV polymerization was demonstrated. The monomer of acrylic acid (AA) can provide the carboxylic groups onto the particles surfaces. Particles carrying surface carboxylic groups are ideal carriers for protein immobilization via reactions between surface carboxylic groups on particles and amino groups of proteins with minimal chemical modification of the protein. The effects of concentration of EGDMA and AA on droplet diameters and the distribution of carboxyl group on particle surfaces were examined. Finally, the bioconjugation of the carboxylated copolymer particles was successfully achieved by first activating the carboxyl groups and incubating with the anti-rabbit IgG–Cy3 conjugates.

2 Design concept

Figure 1 shows the pictures and schematic diagrams of the 2D- and 3D-MFFDs utilizing PDMS to produce

Fig. 1 **a** Schematic diagram of MFFD for production of copolymer particles via in situ UV polymerization by co-flow of aqueous (A) and comonomer (B) phases, **(b)** an image of wetting phenomenon without droplet production occurred in a 2D-MFFD, and **(c–d)** an image and cross section diagram of breakup of liquid tread into droplets in a 3D-MFFD. Fluid A: DI water + 2 wt.% SDS, Fluid B: monomer (ethylene glycol dimethacrylate, EGDMA) + 0–40 wt% acrylic acid (AA) + 4wt% photoinitiator (HCPK, 1-hydroxycyclohexyl phenyl ketone)



monodisperse copolymer particles by means of in situ UV polymerization in a closed microchannel, respectively. For formation of copolymer particles, two immiscible fluids (fluid A: continuous phase, fluid B: disperse phase) were supplied to the MFFD through the $300\ \mu\text{m}$ (W) \times $250\ \mu\text{m}$ (H) rectangular microchannels. Fluid A was a 2 wt.% aqueous solution of sodium dodecyl sulfate (SDS). Fluid B was the monomer mixture of EGDMA with various concentrations of acrylic acid (AA). Four different compositions of comonomer solutions, i.e. EGDMA with $C_{AA}(\text{wt.}\%) = 0, 10, 20, 40\%$ were used in this study. To produce the copolymer particles, we added 4 wt.% of photoinitiator, 1-hydroxycyclohexyl phenyl ketone (HCPK), with the monomer mixture (EGDMA/AA). In the 2D-MFFD configuration, the liquid thread of EGDMA in aqueous solutions tends to stick on the channel wall without droplet breakup due to the high affinity of EGDMA with the hydrophobic PDMS channel surfaces (Fig. 1b). We also tested the comonomer solutions for EGDMA with $C_{AA}(\text{wt.}\%) = 0, 10, 20, 40\%$, and the results showed the same tendency. Therefore, instead of the 2D-MFFD, the proposed 3D-MFFD configuration was used to generate monodisperse comonomer droplets for EGDMA with $C_{AA}(\text{wt.}\%) = 0, 10, 20, 40\%$. The 3D-MFFD device consisted of two slabs of PDMS structures bonded together to form the embedded coaxial orifices (Fig. 1c and d). The embedded coaxial orifices leads to the liquid thread of the fluid B surrounded by fluid A without contact with channel surfaces (Fig. 1d). No wetting was occurred as shown in Fig. 1c. At the flow-focusing orifice, the flow accelerated and subsequently the liquid thread of the fluid B broke into comonomer droplets due to Rayleigh-Plateau hydrodynamic instability

under the competition of viscous and capillary forces (Lin and Reitz 1998). Typical dimensions of the flow-focusing orifice in our devices ranges from 50 to $200\ \mu\text{m}$. By controlling orifice sizes, the production rate and size of comonomer droplets can be varied. The production of copolymer particles was achieved by in situ UV polymerization of the comonomer droplets in the 3D-MFFD. We designed a multiple U-shaped channel to increase the exposure time of the in situ polymerization of the comonomer droplets. The time of photopolymerization was controlled by droplet velocities in a multiple U-shaped channel, generally from 5 s to several minutes. After collection of copolymer particles, the bioconjugation of the carboxylated copolymer particles with the anti-rabbit IgG–Cy3 conjugate were performed by first activating the carboxyl groups and incubating.

3 Experimental

3.1 Fabrication process

Figure 2a shows the schematic diagram of the fabrication process for the 3D-MFFD. The device consisted of two slabs of PDMS structures, which were fabricated using standard soft lithography. Two SU-8 molds (MicroChem, USA) were made on silicon wafer using standard lithography techniques. The SU-8 mold with two layers of SU-8 structures (top left) defined the sizes and shape of the coaxial orifices. The thicknesses of the SU-8 layers were 50 and $60\ \mu\text{m}$. The other mold as a cover (top right) only contained one layer of SU-8 structures with thickness of $60\ \mu\text{m}$. Two separate PDMS layers were cast from the SU-8

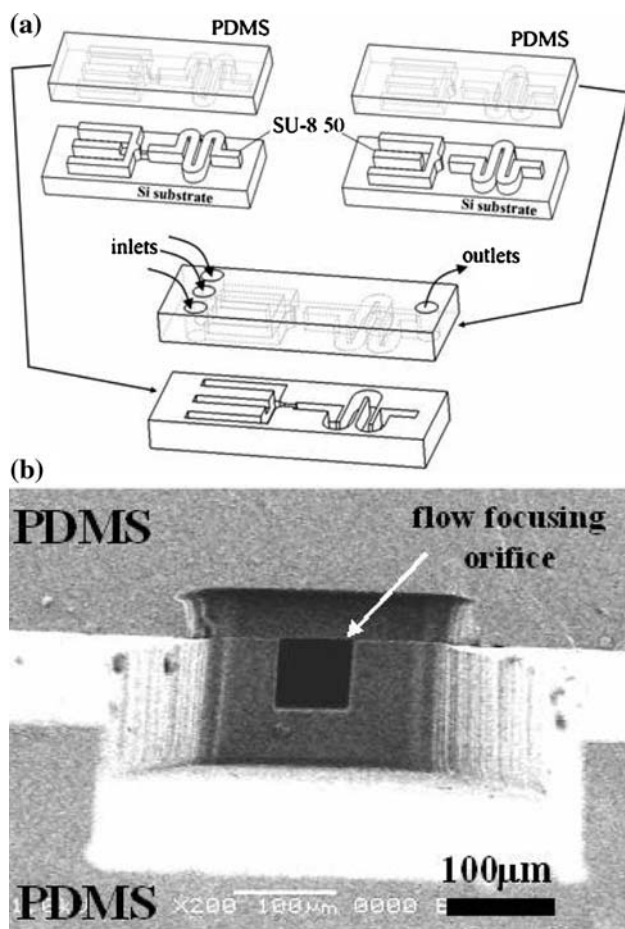


Fig. 2 (a) Schematic diagrams of fabrication processes for the 3D-MFFD, and (b) SEM image of the microfluidic channel with an embedded rectangular orifice measuring $60 \mu\text{m} \times 60 \mu\text{m}$

molds, precisely aligned, and then permanently bonded to form the embedded coaxial orifices after the surfaces treatment with oxygen plasma. The bonding process was operated under a microscope with an alignment error less than $10 \mu\text{m}$. Figure 2b shows the SEM image of the cross section of the microfluidic channel with a rectangular embedded orifice measuring $60 \mu\text{m}$ (W) \times $60 \mu\text{m}$ (H) \times $100 \mu\text{m}$ (L).

3.2 Materials

Monomers, ethylene glycol dimethacrylate (EGDMA), and acrylic acid (AA) were purchased from Aldrich USA.

Other chemicals, sodium dodecyl sulfate (SDS), photoinitiator 1-hydroxycyclohexyl phenyl ketone (HCPK), and 1-ethyl-3-(3-dimethylaminopropyl) carbodiimide hydrochloride (EDC) were obtained from Aldrich USA. *N*-hydroxysulfosuccinimide sodium salt (Sulfo-NHS) was purchased from Fluka USA. Fluorescent solutions of Cy3-conjugated anti-rabbit IgG were purchased and prepared from Chemicon International USA. Four different compositions of comonomer solutions, i.e. EGDMA with $C_{AA}(\text{wt.}\%) = 0, 10, 20, 40\%$ were used in this study. Viscosities of these comonomer solutions were measured by using rotational rheometer (Brookfield Engineering Laboratories, USA). Interfacial tension between the comonomer liquids and a 2 wt.% aqueous solution of SDS was measured by dynamic contact angle analyzer (FTA200, First Ten Angstroms, USA). We injected the comonomer liquid into the static aqueous solution to form a suitably shaped pendant drop using a syringe with a tiny needle. The FTA interfacial tension software was used to fit the actual pendant drop profile. Interfacial tension of two immiscible liquids was calculated according to Laplace–Young equation. The physical properties of EGDMA with $C_{AA} = 0\text{--}40\%$ (wt.%) are given in Table 1. The temperatures of these comonomer solutions are maintained at 25°C for both viscosity and interfacial tension measurements. Besides, the contact angles of comonomer solutions with PDMS surfaces were also measured ranging from 42° to 72° . The results showed that the comonomer liquids have a high affinity with PDMS surfaces.

3.3 Equipment

Liquids were supplied to the device through Teflon tubings connected to syringes (1000 series, Hamilton Co., USA) for the 3D-MFFD in the closed channel configuration. We controlled the flow rates using independent syringe pumps (KDS200, KD Scientific Inc., USA) to provide different flow rates. After changing the flow rates, the device was equilibrated for at least 10 min to ensure stable droplet formation. Photos were recorded by a high-speed video camera (Photron Fastcam-ultima APX, Japan) mounted on an optical microscope (IX-71, Olympus Optical Co. Ltd, Japan). Image processing software (Image-Pro plus, Media Cybernetics Inc., USA) was used to determine droplet

Table 1 Physical properties of EGDMA with $C_{AA} = 0\text{--}40\%$ (wt.%)

EGDMA + C_{AA} (wt.%)	Viscosity μ (cP)	Interfacial tension with DI water γ (mN/m)	μ/γ	Contact angles on PDMS surfaces
0	6.5	5.7	1.14	42
10	5.7	5.1	1.12	48
20	4.8	4.4	1.09	57
40	3.4	3.2	1.06	72

sizes. For synthesis of copolymer particles, we carried out the in situ UV polymerization of the comonomer droplets using an optical microscope (IX-71) equipped with a 100 W mercury lamp and a filter set for UV light irradiation at 330–380 nm.

3.4 Procedures of Bioconjugation of copolymer particles

The EDC/sulfo-NHS mixture of 3.9 mg EDC and 1.1 mg sulfo-NHS dissolved in a 1 ml of 0.1 M sodium phosphate buffer at pH 7.4 were prepared. EDC is the most popular carbodiimide used in conjugating biological substances. Sulfo-NHS is used to modify a carboxyl group to an amine-reactive ester. The advantage of adding sulfo-NHS to EDC reactions is to increase the stability of the active intermediate (Sinz 2006) during the process of biological conjugation. The bioconjugation of the copolymer particles was achieved by first dispersing them in the 100 μ l of EDC/sulfo-NHS mixture to activate the carboxyl groups on particle surfaces at room temperature for 1 h. Following this step, 100 μ l of the 10^{-3} mg/ml Cy3-conjugated anti-rabbit IgG (Cy3-IgG) solution in 0.1 M sodium phosphate buffer was added to attach (Cy3-IgG) to particles through the carboxyl groups on particle surfaces at room temperature for 1 h. After depositing the copolymer particles and removing excess Cy3-IgG solution, we resuspended them in the deionized water, and observed the fluorescent distribution of the particle surfaces on a glass slide under a microscopy.

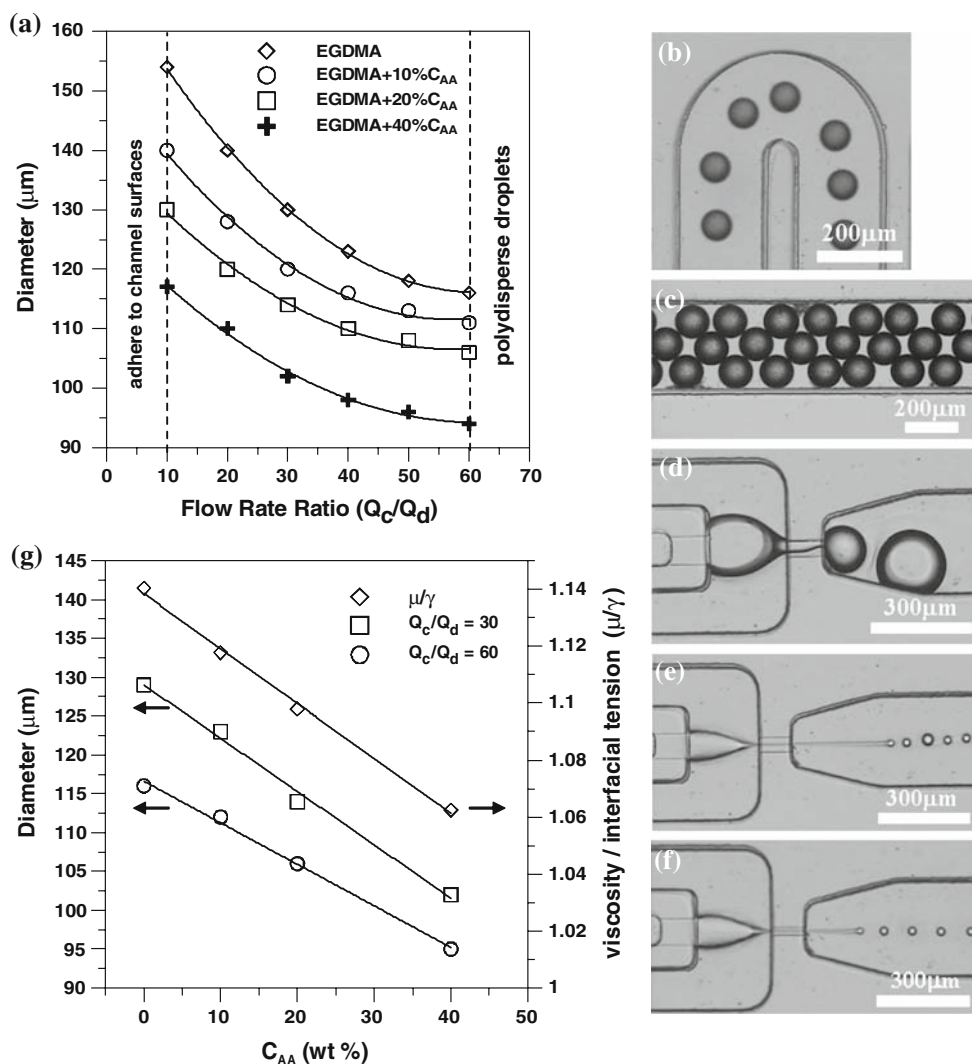
4 Results and discussions

4.1 Formation of copolymer particle in the 3D-MFFD

To demonstrate the synthesis of copolymer particles in the 3D-MFFD, we used the monomer mixture (EGDMA/AA) with $C_{AA} = 0$ to 40% wt.%. No leakage was observed within the range of flow rates tested. The swelling of PDMS caused by the comonomer solutions was not apparent during the experiments. Figure 3a shows the variation in droplet diameters with the change of the ratio of flow rates (Q_c/Q_d). By varying the flow rate of the continuous phase (Q_c) while keeping the flow rate of dispensed phase (Q_d) constant at 1 μ l/min, comonomer droplets ranging from 95 to 155 μ m were produced. The dimensions of droplets were controlled by the ratio of flow rates (Q_c/Q_d) and the properties of monomer mixture [that is, its viscosity (μ) and interfacial tension (γ) with a continuous phase]. At the range of $(Q_c)/(Q_d) = 10$ –60, we observed the monodisperse droplets were generated by breaking up the comonomer thread in or behind the orifice without satellite

droplets produced. Although the comonomer liquid has a high affinity with PDMS microchannels as shown in Table 1, the comonomer fluid threads for EGDMA with $C_{AA} = 0$ –40% can be clearly observed through the flow-focusing orifice, and break into droplets (Fig. 1c). No wetting phenomenon was occurred, indicating that the affinity of the dispensed phase with the material of the microchannels has no influence on droplet formation. The droplets aligned as a chain of droplets near the central axis without coalescence and passed through the U-shaped microchannels under UV light irradiation (Fig. 3b). Figure 3c shows a photograph of the aggregation of the copolymer particles after in situ UV polymerization. We measured the size distribution of the formed copolymer particles (at least 90 particles) for EGDMA with $C_{AA} = 0$ –40% at the range of $(Q_c)/(Q_d) = 10$ –60 showing the coefficient of variance (C.V.) less than 5%. C.V. is defined as the ratio between the standard deviation of the diameter and the mean diameter. A C.V. of less than 5% is the commonly accepted definition of monodispersity. However, for $(Q_c)/(Q_d) < 10$, we found that the comonomer thread has a trend to wet the top/bottom channel surfaces and adhere to the orifice causing the droplets growing, so that the large droplets were produced after the droplets broke up (Fig. 3d). This wetting phenomenon was observed for all the cases of $C_{AA} = 0$ –40% at $(Q_c)/(Q_d) < 10$. It is due to the fact that the continuous phase cannot effectively surround all the comonomer thread after the disperse phase passed through the inner fluid orifice at low ratio of flow rates. Besides, for $(Q_c)/(Q_d) > 60$, we found that a transition to the jetting mode occurred (Seo et al. 2005b). The comonomer thread passing through the flow-focusing orifice broke up into main population of droplets accompanied with small satellite droplets (Fig. 3e). Although the droplet sizes smaller than 50 μ m can be observed at higher ratio of flow rates, i.e. ($Q_c/Q_d > 100$), the polydispersed distribution of droplet sizes did not satisfy the needs in biological applications. To produce the monodisperse droplet sizes smaller than 50 μ m, we reduced the rectangular orifice sizes with a cross section of 30 μ m (W) \times 30 μ m (H) and operated at proper ratio of flow rates. We successfully demonstrated the generation of the monodisperse droplet sizes ranging from 10 to 90 μ m. Figure 3f shows the production of the monodisperse droplets with diameter of 20 μ m operated at a ratio of flow rates $Q_c/Q_d = 140$ and $Q_d = 0.4$ μ l/min. The droplet sizes smaller than 50 μ m, approaching 10 μ m, can be generated, but the control of flow rates to produce stable monodisperse droplets becomes difficult due to the smaller orifice sizes. For a particular ratio of flow rates, we found that an increase in C_{AA} from 0 to 40 wt.% resulted in a notable decrease in the droplet diameters. Figure 3g shows the effect of composition of the EGDMA/AA mixture on droplet dimension at $(Q_c)/(Q_d) = 30$ and 60 as well

Fig. 3 (a) Variation in droplet diameter plotted versus the ratio of flow rates of aqueous (Q_c) and monomer (Q_d) phases. Q_d is fixed at $1 \mu\text{l}/\text{min}$. (b) An image of comonomer droplets flowing in the multiple U-shaped-channel used for in situ UV polymerization. (c) Typical image of EGDMA/AA microspheres after in situ UV polymerization. (d) Typical image of the comonomer thread adhering to the orifice without breakup of a droplets for $(Q_c)/(Q_d) < 10$. (e) Typical image of the comonomer thread break up into main population of droplets accompanied with small satellite droplets for $(Q_c)/Q_d > 60$. (f) Typical image of the production of the monodisperse droplets with diameter of $20 \mu\text{m}$ operated at a ratio of flow rates $Q_c/Q_d = 140$, and the rectangular orifice sizes with a cross section of $30 \mu\text{m}$ (W) \times $30 \mu\text{m}$ (H). (g) Variation in droplet diameter at $Q_c/Q_d = 30$ and 60 as well as the ratio of viscosity (μ) and interfacial tension (γ) with respective to the composition of the EGDMA/AA mixtures, respectively



as the ratio of viscosity (μ) and interfacial tension (γ), respectively. By fixing the ratio of flow rates, the sizes of comonomer droplets has an appropriately linear decrease as increasing C_{AA} (wt.%) from 0 to 40%. We attributed this effect to that the increase of C_{AA} (wt.%) can cause the decrease of comonomer viscosity and interfacial tension with the continuous phase (Table 1). The ratio (μ/γ) of viscosity and interfacial tension also showed an appropriately linear decrease as increasing C_{AA} (wt.%) from 0 to 40% as shown in Fig. 3g. The decrease of droplet dimension corresponding to the decrease of the ratio (μ/γ) can be explained via a capillary number $Ca = \mu v/\gamma$, where v is the characteristic velocity of the aqueous phase. Increasing Ca results in the decrease of the droplet diameters, accordingly (Seo et al. 2005a). At a fixed characteristic velocity (v), the ratio (μ/γ) dominates the decrease of the droplet diameters. The results are consistent with the previous report for synthesis of copolymer particles (TGDMA/AA) in PU-based 2D MFFD (Lewis et al. 2005). Besides, as increasing C_{AA} (wt.%) from 0 to 40%, we found that more time was

needed to completely solidify the comonomer droplets. For the case of C_{AA} (wt.%) $> 40\%$, the incompletely solidified particles had a trend to adhere to the microchannel surfaces causing the microchannel clogging.

4.2 Bioconjugation of copolymer particles with anti-rabbit IgG–Cy3 conjugates

Figure 4a and b shows a typical photographs and fluorescent images of the IgG–Cy3 conjugated copolymer particles. A control experiment for the polymer particles with $C_{AA} = 0\%$; i.e. EGDMA only, was conducted to prove that IgG–Cy3 attached to the copolymer microsphere surfaces via reaction between carboxyl group on particle surfaces and amino group of protein. No fluorescence was observed for the polymer particles (EGDMA only) after performing the bioconjugated processes. For the copolymer particles with $C_{AA} = 10\%$, we can clearly observe the fluorescent signal from the particle surfaces indicating that the carboxylic groups on the surface of the copolymer

particles can provide the functional groups for the immobilization of biomolecules (Fig. 4a). Bioconjugation of EGDMA/AA particles with anti-rabbit IgG–Cy3 conjugates was successfully demonstrated. However, non-uniform distribution of fluorescence on the copolymer particle surfaces was observed for EGDMA with $C_{AA} = 10\%$. We attribute to the factors of EGDMA with a low C_{AA} and the water-soluble AA diffusing from the monomer mixture into the aqueous phase. Therefore, we attempted to increase the composition of C_{AA} from 10 to 40% to improve the distribution of fluorescence on the copolymer particle surfaces as shown in Fig. 4b. Uniform distribution of fluorescence on the copolymer particle surfaces was observed. Figure 4c shows the surface fluorescent distribution and diameter variation of the bioconjugated copolymer particles on the effect of the composition C_{AA} . The surface fluorescent distribution of the bioconjugated copolymer particles was calculated as the coefficient of variance (C.V.). The C.V. defined as the ratio of the standard deviation to the mean of the pixel intensity values on copolymer particle surfaces, and at least 60 particles were examined. The decrease of the C.V. indicates the improvement of the uniform fluorescent distribution on the copolymer particle surfaces. By increasing the concentration of C_{AA} from 10 to 40% accompanied with decreasing the microsphere sizes, high efficiency of bioconjugation on carboxylated copolymer particles was achieved.

To simply examine the penetration depth of antibodies (IgG–Cy3 conjugates) within the copolymer particles, we deposited a series of 0.1 μl comonomer droplets of EGDMA with $C_{AA} = 10, 20, 40\%$ onto a glass slide. After the procedures of UV polymerization and bioconjugation with anti-rabbit IgG–Cy3 conjugates as described in Sect. 3.4,

the hemispherical copolymer particles with diameter of 800 μm were produced on a glass slide. We focused on the plane at the bottom surface of hemispherical copolymer particles, and observed the fluorescent distribution using an inverted microscopy with the depth of field about 10 μm (Fig. 5a). For the hemispherical copolymer particles with $C_{AA} = 10\%$, only weak fluorescent light near the bottom surface edge of the copolymer particles was observed (Fig. 5b). The penetration depth of anti-rabbit IgG–Cy3 was approximately about 10 μm measuring from the edge of the bottom surfac. However, the penetration depth of anti-rabbit IgG–Cy3 within the hemispherical copolymer particles significantly increased from 40 to 100 μm for EGDMA with $C_{AA} = 20$ and 40%, respectively (Fig. 5c, d). The results explicitly indicate that the fluorescent-labeled antibodies are not only conjugated on the external surface of the copolymer particles, but can also penetrate into the copolymer particles. We attribute this phenomenon to two contributing factors: (a) the content of AA buried within copolymer particles and (b) the poly(EDGMA-co-AA) network size. First, this should be pretty straightforward that increasing the AA concentration results in a higher content of AA buried within the copolymer particle. As the anti-rabbit IgG–Cy3 diffuses inside the copolymer particle, a higher content of the anti-rabbit IgG–Cy3 conjugates is immobilized via AA functional groups within copolymer particles. Second, increasing the AA concentration results in the increase of the poly(EDGMA-co-AA) network sizes, which can increase the possibility of the anti-rabbit IgG–Cy3 diffusing into the copolymer particles.

To examine the cross-linked network structures of the poly(EDGMA-co-AA) network, we sliced and observed

Fig. 4 Schematic and typical fluorescent images of the copolymer particles conjugated with IgG–Cy3 for (a) $C_{AA} = 10$ wt%, and (b) $C_{AA} = 40$ wt%. (c) Variation in surface fluorescent distribution and diameters of the bioconjugated copolymer particles with respective to the composition of C_{AA} (wt.%)

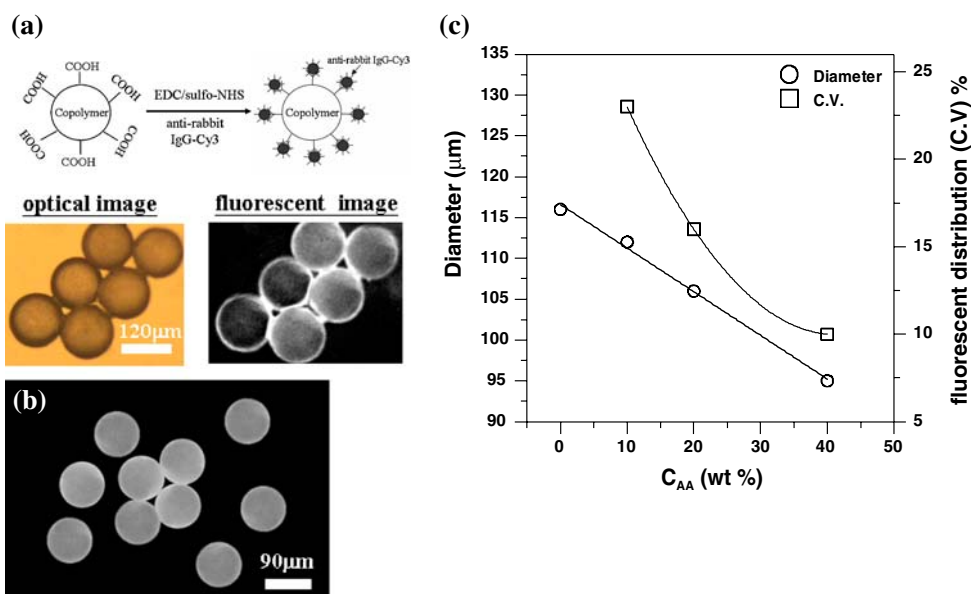
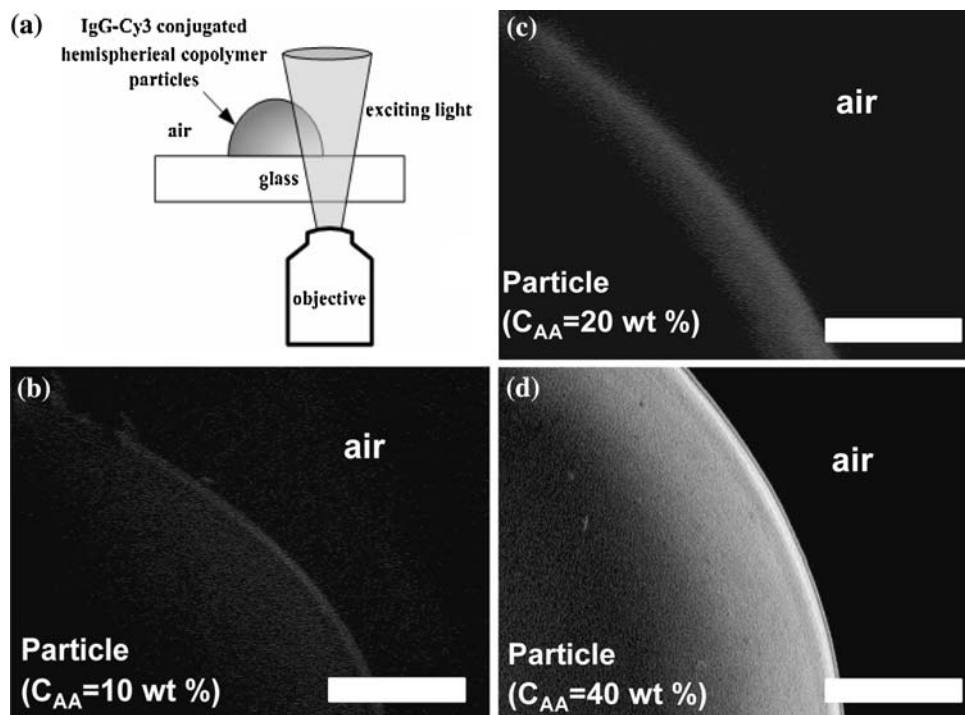


Fig. 5 (a) Schematic diagram of the penetration depth measurements of anti-rabbit IgG–Cy3 conjugates within the hemispherical copolymer particles produced and on a glass slide. (b–d) Typical fluorescent images on the bottom surface of the hemispherical copolymer particles conjugated with IgG–Cy3 for (b) $C_{AA} = 10$ wt.%, (c) $C_{AA} = 20$ wt.%, and (d) $C_{AA} = 40$ wt.%, respectively. (Scale bars indicate $100\ \mu\text{m}$)



within the hemispherical copolymer located near the particle surfaces by means of a scanning electron microscope. Figure 6a and b shows the SEM images of the cross-linked poly(EDGMA-co-AA) network structures within the hemispherical copolymer particles for EGDMA with $C_{AA} = 10$ and 40%, respectively. Compared with EGDMA with $C_{AA} = 10\%$, the cross-linked network structures for $C_{AA} = 40\%$ are apparently less dense than that of $C_{AA} = 10\%$ inside the copolymer particles. The results indicate that increasing the AA concentration results in the decrease of the cross-linked density, i.e. larger network mesh size, which can increase the possibility of the anti-rabbit IgG–Cy3 diffusing into the copolymer particles. The detailed structure and degree of polymerization of the poly(EDGMA-co-AA) network within the copolymer particles with respect to varying AA compositions as demonstrated in the present study are complicated and is beyond the scope of this paper, but the effect of the mixing ratio of the comonomer liquids of EGDMA and AA on the network density may be comparable with the previous literature (Jiu J et al. 2002) in the cross-linked density. They found that the increased ratio of copolymer gel of hydroxyl ethyl methacrylate (HEMA) and EGDMA where the latter worked as the crosslinker can decrease the cross-linked density characterized by Fourier Transform Infrared Spectrometer (FT-IR). Therefore, as the AA concentration is increased, higher content of AA will be buried within the copolymer particles and larger network mesh sizes of the poly(EDGMA-co-AA) network will also be generated, resulting in a higher degree of anti-rabbit IgG–Cy3

immobilization within the copolymer particles. Increasing the concentration of C_{AA} from 10 to 40% exhibits high efficiency of bioconjugation on carboxylated copolymer particles, which is consistent with the previous results shown in Fig. 4. Besides, the increase of AA concentration could probably alter the mechanical stretch of the copolymer particles due to the change of the cross-linked network structures. No deformation of the copolymer particles was observed after many times of collision between particles and under high flow rates. It seems to have no detrimental impacts on the potential uses in biotechnology applications, but more detailed study is needed.

5 Conclusion

We produced monodisperse copolymer (EGDMA/AA) particles carrying surface carboxyl groups using a planar 3D-MFFD in a closed microfluidic system. As the dispensed phase does not contact the channel walls, we can produce monodisperse comonomer droplets with a C.V. of less than 5% without any surface modifications of the channel walls. In situ UV polymerization of comonomer droplets was performed to form the copolymer particles. By controlling device configuration and pumping flow rates, we believe that it is possible to form monodisperse copolymer particles ranging from few microns to few hundred-micron sizes in the proposed 3D-MFFD. Bioconjugation of EGDMA/AA particles with anti-rabbit IgG–Cy3 conjugates was successfully demonstrated. By

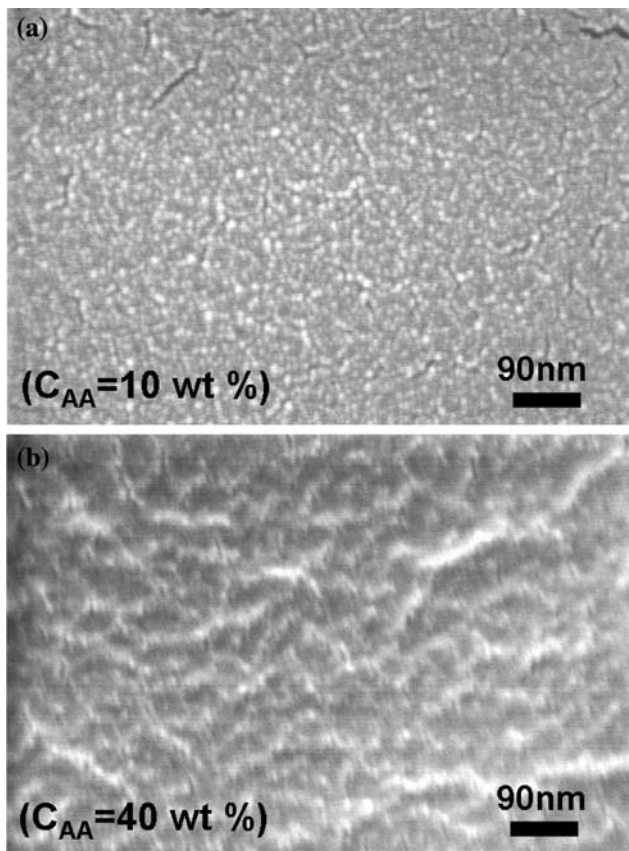


Fig. 6 SEM images of the crosslinked poly(EDGMA-co-AA) network structures within the hemispherical copolymer particles for EGDMA with (a) $C_{AA} = 10\%$ and (b) $C_{AA} = 40\%$

increasing the concentration of C_{AA} (wt.%) accompanied with decreasing the microsphere sizes, high efficiency of bioconjugation on carboxylated copolymer particles was achieved. Our proposed approach is not limited by the selection of comonomer liquids of EGDMA/AA used in this study. Other polymer/copolymer particles, such as TPGDA, TPGDA/AA or TPGDA mixed with amino ethyl methacrylate (AEMA) for functionalization of the particles with-NH₂ groups, can be produced, if interfacial tension and the ratios of fluid viscosities allow for its formation. The rapid continuous synthesis of carboxylated copolymer particles via a microfluidic device provides a reliable control of particle sizes and composition for massive production in biotechnological applications.

Acknowledgments This work was partially supported by National Science Council, Taiwan, through the grant NSC 97-2218-E-019-001-MY2.

References

Arshady R (1992) Suspension, emulsion, and dispersion polymerization: a methodological survey. *Colloid Polym Sci* 270:717–732

- Arshady R (1993) Microspheres for biomedical applications: preparation of reactive and labelled microspheres. *Biomaterials* 14:218–224
- Banderas ML, Mosquera FM, Chueca RP, Rodriguez AG, Cebolla A, Chavez S, Ganan Calvo AM (2005) Flow focusing: a versatile technology to produce size-controlled and specific-morphology microparticles. *Small* 1:688–692
- Dendukuri D, Tsoi K, Hatton TA, Doyle PS (2005) Controlled synthesis of nonspherical microparticles using microfluidics. *Langmuir* 21:2113–2117
- Huang SH, Tan WH, Tseng FG, Takeuchi S (2006) A monolithically three-dimensional flow-focusing device for formation of single/double emulsions in closed/open microfluidic systems. *J Micro-mech Microeng* 16:2336–2344
- Jiu J, Kurumada KI, Tanigaki M (2002) Preparation of nanoporous silica using copolymer template. *Mater Chem Phys* 78:177–183
- Jeong WJ, Kim JY, Choo J, Lee EK, Han CS, Beebe DJ, Seong GH, Lee SH (2005) Continuous fabrication of biocatalyst immobilized microparticles using photopolymerization and immiscible liquids in microfluidic systems. *Langmuir* 21:3738–3741
- Kesenci K, Kin EP (1998) Production of poly (ethylene glycol dimethacrylate)-coacrylamide based hydrogel beads by suspension copolymerization. *Macromol Chem Phys* 199:385–391
- Kawaguchi H (2000) Functional polymer microspheres. *Prog Polymer Sci* 25:1171–1210
- Lin SP, Reitz RD (1998) Drop and spray formation from a liquid jet. *Annu Rev Fluid Mech* 30:85–105
- Lewis PC, Graham RR, Nie Z, Xu S, Seo M, Kumacheva E (2005) Continuous synthesis of copolymer particles in microfluidic reactors. *Macromolecules* 38:4536–4538
- Loscertales IG, Barrero A, Guerrero I, Cortijo R, Marquez M, Ganan Calvo AM (2002) Micro/nano encapsulation via electrified coaxial liquid jets. *Science* 295:1695–1698
- Nie Z, Xu S, Seo M, Lewis PC, Kumacheva E (2005) Polymer particles with various shapes and morphologies produced in continuous microfluidic reactor. *J Am Chem Soc* 127:8058–8063
- Nie Z, Li W, Seo M, Xu S, Kumacheva E (2006) Janus and ternary particles generated by microfluidic synthesis: design, synthesis, and self-assembly. *J Am Chem Soc* 127:8058–8063
- Nisisako T, Torii T (2007) Formation of biphasic janus droplets in a microfabricated channel for the synthesis of shape-controlled polymer microparticles. *Adv Mater* 19:1489–1493
- Nisisako T, Torii T, Higuchi T (2002) Droplet formation in a microchannel network. *Lab Chip* 2:24–26
- Nisisako T, Torii T, Higuchi T (2004) Novel microreactors for functional polymer beads. *Chem Eng J* 101:23–29
- Nisisako T, Torii T, Takahashi T, Takizawa Y (2006) Synthesis of monodisperse bicolored janus particles with electrical anisotropy using a microfluidic co-flow system. *Adv Mater* 18:1152–1156
- Oh HJ, Kim SH, Baek JY, Seong GH, Lee SH (2006) Hydrodynamic micro-encapsulation of aqueous fluids and cells via on the fly photopolymerization. *J Micromech Microeng* 16:285–291
- Okushima S, Nisisako T, Torii T, Higuchi T (2004) Controlled production of monodisperse double emulsions by two-step droplet breakup in microfluidic devices. *Langmuir* 20:9905–9908
- Rembaum A, Toke ZA (1998) *Beads: medical and biological applications*. CRC Press, Boca Raton
- Slomkowski S (1998) Polyacrolein containing microspheres: synthesis, properties and possible medical applications. *Prog Polymer Sci* 23:815–874
- Seo M, Nie Z, Xu S, Lewis PC, Kumacheva E (2005a) Microfluidics: from dynamic lattices to periodic arrays of polymer disks. *Langmuir* 21:4773–4775

- Seo M, Nie Z, Xu S, Mok M, Lewis PC, Graham R, Kumacheva E (2005b) Continuous microfluidic reactors for polymer particles. *Langmuir* 21:11614–11622
- Seong GH, Heo J, Crooks RH (2003) Measurement of enzyme kinetics using a continuous-flow microfluidic system. *Anal Chem* 75:3161–3167
- Sinz A (2006) Chemical cross-linking and mass spectrometry to map three-dimensional protein structures and protein–protein interactions. *Mass Spectrom Rev* 25:663–682
- Takeuchi S, Garstecki P, Weibel DB, Whitesides GM (2005) An axisymmetric flow-focusing microfluidic device. *Adv Mater* 17:1067–1072
- Utada AS, Lorenceau E, Link DR, Kaplan PD, Stone HA, Weitz DA (2005) Monodisperse double emulsions generated from a microcapillary device. *Science* 308:537–541
- Zhang H, Huang H, Lv R, Chen RHM (2005) Micron-size crosslinked microspheres bearing carboxyl groups via dispersion copolymerization. *Colloids Surf A Physicochem Eng Aspects* 253:217–221